REVIEW

Frontiers in Ultrashort Pulse Generation: Pushing the Limits in Linear and Nonlinear Optics

G. Steinmeyer,* D. H. Sutter, L. Gallmann, N. Matuschek, U. Keller

Optical pulses in the 5-femtosecond range are produced by a variety of methods. Although different in technical detail, each method relies on the same three key components: spectral broadening due to the nonlinear optical Kerr effect, dispersion control, and ultrabroadband amplification. The state of the art of ultrashort pulse generation is reviewed with a focus on direct laser oscillator schemes.

Our ability to perceive the dynamics of nature is ultimately limited by the temporal resolution of the instruments available to us. Mechanical shutters allow for resolution in the millisecond range, whereas stroboscopic illumination allows us to probe the microsecond range. Modern electronic sampling oscilloscopes eventually brought the limit down into the picosecond range. Ultrafast lasers have advanced the temporal resolution of measurements another three orders of magnitude into the sub–10-fs (1 fs = 10^{-15} s) regime, allowing for the direct observation of vibrational molecular dynamics (*1*). The broad spectral content can be used in medical diagnostics (*2*), and the extreme concentration of energy in femtosecond pulses is useful for material processing because much finer structures can be created in the absence of thermal interaction caused by longer pulses (*3*).

Figure 1 shows the historical development of ultrafast pulse generation. In the late 1980s, the pulse duration of dye lasers was as low as 27 fs (*4*), which was later compressed to 6 fs (*5*). At a wavelength of 600 nm, only three optical cycles fit under the full width at half maximum of the intensity envelope of such a pulse. It took almost a decade to surpass these results with solid-state lasers. Our goal is to review this recent progress with ultrafast solid-state lasers.

Measurement of ultrashort pulses is also a demanding task. Whereas traditionally, a short event has been characterized with the aid of an even shorter event, this is not an option for the characterization of the shortest event. Nonlinear autocorrelation techniques have been used in ultrafast optics because they use a short event to measure itself. In this type of measurement, two replicas of the pulse are generated, which are delayed with respect to each other. An instantaneous nonlinear optical effect, such as second-harmonic generation or two-photon absorption, is used to form the product of the two replicas, which depends on the temporal overlap of the replicas. Effectively, this allows converting measurement of a time into the measurement of a distance. Examples of autocorrelation measurements of some of the shortest pulses generated to date are shown (Fig. 2). Although completely different pulse generation techniques were employed in these examples, the autocorrelation traces are very similar, as indicated by the relative magnitude of the first- and second-side maximum of the traces shown.

Here, we describe methods that can be used to generate pulses as short as those displayed in Fig. 2, with a full width at half maximum of only about 5 fs (*6–10*). For a wavelength in the visible or near-infrared spectral range, as in the examples we discuss, this corresponds to about two optical cycles. We will show that pulse generation techniques demonstrated in the two-cycle regime rely essentially on three identical ingredients: the nonlinear optical Kerr effect acting as a spectral broadening process, precise control of dispersion, and an ultrabroadband amplifying process. Here, we review these key ingredients comprehensively and focus on the interaction between nonlinear pulse-shaping processes and linear phase correction. We emphasize how these effects can be used inside a laser to directly generate extremely short pulses.

The Kerr Effect, Dispersion, and Pulse Compression

At high intensities, the polarization inside a dielectric medium does not proportionally follow the electric field, and a nonlinear component at the frequency of the exciting wave is induced, giving rise to an instantaneous change of the refractive index n proportional to the time- and space-dependent intensity $I(t, \vec{x})$

$$n(t,\vec{x}) = n_0 + n_2 I(t,\vec{x}) \qquad (1)$$

This is called the optical Kerr effect (*11*), which is essential for all the concepts delivering pulses in the two-cycle regime. For typical solid-state materials, the nonlinear index n_2 is on the order of several 10^{-16} cm^2/W. The index change causes a temporal delay or phase shift for the most intense parts of a beam. Assuming Gaussian spatial and temporal profiles, the effects caused by this index change are shown (Fig. 3) longitudinal and transverse to the propagation direction. Retardation of the most intense part of a plane wavefront transversely acts like a focusing lens, whereas along the axis of propagation, the Kerr effect retards the center of an optical pulse. This longitudinal effect produces a red shift of the leading part of the pulse, and a blue shift in the trailing part and has also been named self-phase modulation (SPM). It is important to note that SPM generates extra bandwidth, that is, it spectrally broadens the pulse.

SPM alone does not modify the pulse envelope, but a much shorter pulse can be created with the extra bandwidth generated, as follows from the Fourier transform of the wider spectrum. To exploit the broadened bandwidth for the generation of a shorter pulse, the red and blue components in the temporal wings of the pulse have to be temporarily delayed and advanced, respectively. The spectral dependence of the speed of light needed to shorten the

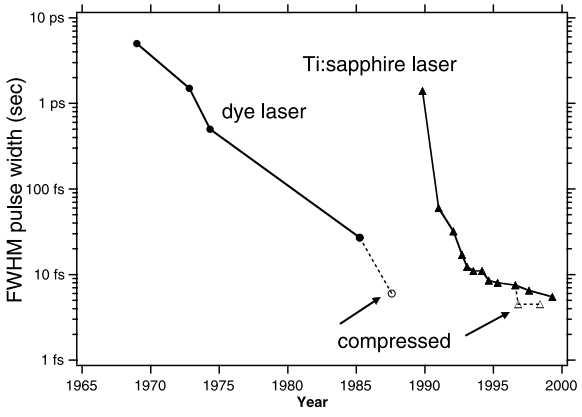

Fig. 1. Development of shortest reported pulse duration over the last three decades. Circles refer to dye-laser technology, triangles refer to Ti:sapphire laser systems. Filled symbols indicate results directly achieved from an oscillator, open symbols indicate results achieved with additional external pulse compression.

Institute of Quantum Electronics, Swiss Federal Institute of Technology, ETH Hönggerberg, HPT, CH-8093 Zürich, Switzerland.

*To whom correspondence should be addressed. E-mail: sguenter@iqe.phys.ethz.ch

spectrally broadened pulse is called dispersion, which is a linear optical effect independent of intensity. For a given optical element with length ℓ, dispersion manifests itself as a spectrally dependent propagation time. Spectral components at (angular) frequency ω are delayed by a group delay

$$T_g(\omega) = \frac{\ell}{c}\frac{\partial}{\partial\omega}(\omega n)$$

$$= \sum_{i=0}^{\infty} \frac{1}{i!}\frac{\partial^i T_g}{\partial\omega^i}\bigg|_{\omega_0} (\omega - \omega_0)^i \qquad (2)$$

where c is the speed of light in vacuum, and ω_0 is a reference frequency for series expansion. The first coefficient ($i = 1$ in Eq. 2) in this dispersion series $\partial T_g(\omega_0)/\partial\omega$ is also called group delay dispersion (GDD), which is a function of reference frequency. A careful balance between frequency dependence given by dispersion and time dependence given by nonlinearity of the refractive index n is needed for efficient compression of a pulse. In most compression schemes, nonlinearity and dispersion are supplied in two successive steps, but optical fibers in the infrared provide these two effects simultaneously. This gives rise to solitons, optical pulses that are able to propagate for long distances in a nonlinear medium with either a constant or a periodically changing pulse shape (*11, 12*).

Ultimately, compression schemes are limited by higher-order dispersion (terms with $i > 1$ in Eq. 2) and parasitic nonlinearities. For pulses shorter than 100 fs, compression is typically limited to factors of less than 10: Dye laser pulses with 50 fs duration have been compressed down to 6 fs (*5*). Similar concepts have been used for external pulse compression of 13-fs pulses from a Ti:sapphire laser (*9*) and of 20-fs pulses from a Ti:sapphire laser amplifier (*10*), resulting in both cases in approximately 4.5-fs pulses (Fig. 2). The use of a hollow fiber filled with a noble gas resulted in unsurpassed pulse energies of about 0.5 mJ with 5.2-fs pulses and a peak power of 0.1 TW (*13*).

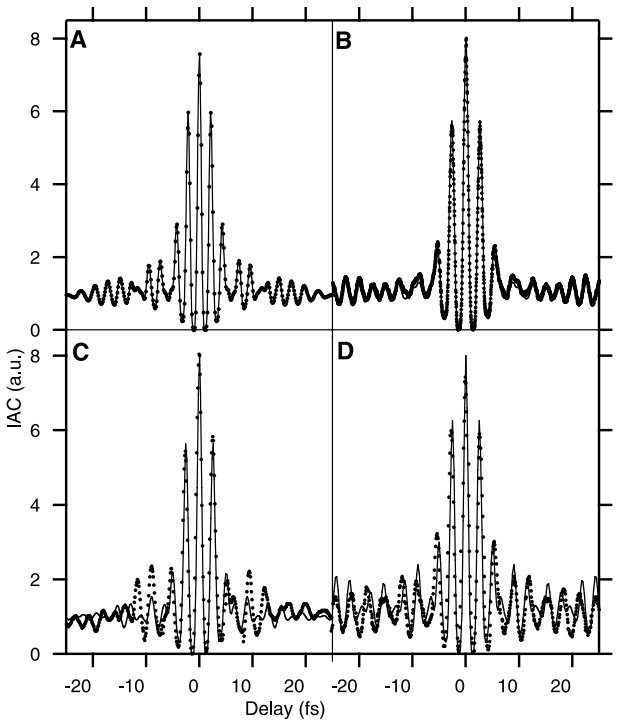

Fig. 2. Comparison of interferometric autocorrelation traces of different pulse sources in the 5-fs range. (**A**) Optical parametric amplification (*8*), (**B**) compression of cavity-dumped pulses in a silica fiber (*9*), (**C**) compression of microjoule pulses in a hollow fiber filled with krypton (*10*), and (**D**) pulses from a Ti:sapphire oscillator (*7*). Dots in (A) through (D) and lines in (A) refer to measured data, lines in (B) through (D) indicate the fit that was used to estimate pulse duration from the autocorrelation.

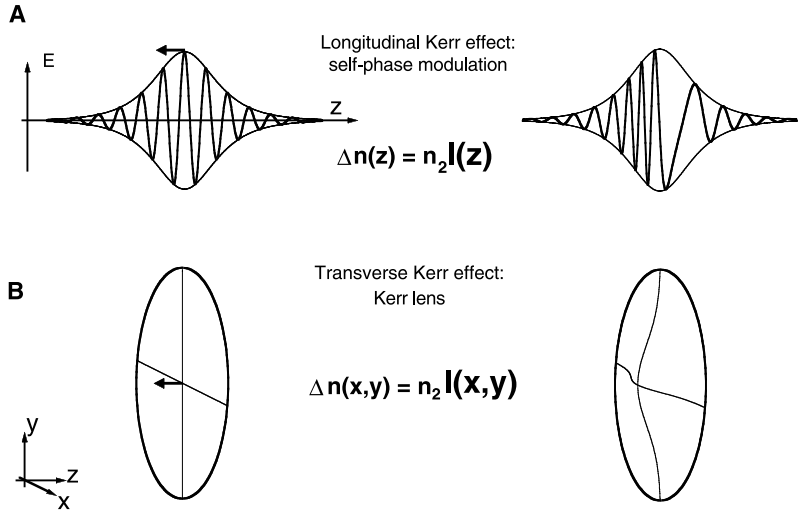

Fig. 3. The Kerr effect gives rise to an increase of the refractive index with intensity, causing a retardation of the most intense parts of a pulse. In its longitudinal form (**A**), the Kerr effect causes self-phase modulation; in its transverse form (**B**), a nonlinear lens is formed in the central part of the beam profile.

Saturable Absorbers and Passive Mode-Locking

A compression scheme can be directly integrated into a laser. In this section, we describe how to place a suitable nonlinear optical device in the feedback loop of the laser oscillator to directly support short-pulse operation (Fig. 4A). Traditionally, this type of operation of a laser has often been considered in the frequency domain (*14*). In this picture, the eigenfrequencies (or longitudinal modes) of the cavity have to be phase-locked to generate a short pulse. An amplitude modulator inside the cavity phase-locks these longitudinal modes when the modulation frequency is equal to the frequency spacing of the modes. This type of operation has been named mode-locking. In the time-domain picture, mode-locking means that the amplitude modulator opens and closes synchronously with the light propagating through the cavity. The modulator can either be driven by an external signal source (active mode-locking) or directly by the optical pulses inside the laser cavity (passive mode-locking). Here, we restrict ourselves to the latter method because it delivers the shortest pulses. The goal is to phase-lock as many longitudinal modes as possible because the broader the phase-locked spectrum the shorter the pulse that can be generated.

The passive amplitude modulator is a saturable absorber which has an increased transmission or reflection for high peak powers and produces a self-amplitude modulation (SAM). This SAM reduces the losses for short-pulse operation of a laser. An optical pulse traveling through a saturable absorber in a solid-state laser is shortened by the SAM, provided the response time of the absorber is sufficiently fast. In a mode-locked laser, pulse formation should start from normal noise fluctuations in the laser to initiate mode-locking. In the steady-state femtosec-

ond regime, dispersion and bandwidth limitation of the gain medium, mirrors, and so forth mainly cause temporal stretching of the pulse. Therefore, the pulse shortening effect must be dominant for pulse durations ranging from nanoseconds at start-up to femtoseconds at steady-state operation.

Traditionally, dyes have been used as saturable absorbers for passive mode-locking. Today in solid-state lasers, dyes have either been replaced by saturable absorbers obtained by Kerr or semiconductor nonlinearities. The precise control of optical nonlinearities, combined with the availability of a variety of bandgaps ranging from the visible to the infrared, makes semiconductor materials very attractive for use as saturable absorbers in solid-state lasers (*15*). Semiconductor materials typically provide an optical nonlinearity with two pronounced time constants. Intraband processes give rise to a very rapid relaxation in the 100-fs regime, while electron-hole recombination generates a slow response time in the picosecond regime. The slow response time can be reduced by several orders of magnitude with low-temperature epitaxy (*16*). Such semiconductors grown at low temperatures are markedly different from normally grown materials, exhibiting an increase in trap densities and decrease in carrier lifetimes of four orders of magnitude. The ability to artificially vary such parameters allowed a systematic study of pulse generation. Typically, a semiconductor saturable absorber is integrated directly into a mirror structure, resulting in a device whose reflectivity increases as the incident optical intensity increases. This general class of devices is called semiconductor saturable absorber mirrors (SESAMs) (*15*). With SESAMs, all important saturable absorber parameters, such as response time, saturation fluence, and modulation depth, can be adapted over several orders of magnitude. This allowed for the first demonstration of self-starting and stable passive mode-locking of diode-pumped solid-state lasers with intracavity saturable absorbers (*17*). The mirror structure can be manufactured using semiconductor materials (for example, AlAs/AlGaAs), standard dielectric coating materials, or a metal coating. So far, metal mirror–based SESAMs demonstrate the largest bandwidth but also limit the average output power (*18*). Schemes using broadband AlGaAs/CaF_2 Bragg mirrors are being considered as well (*19*).

The extremely rapid response and the broad bandwidth of the Kerr nonlinearity are very attractive for a mode-locking process. One way of using the phase nonlinearity of the Kerr effect for mode-locking is to convert SPM into an effective amplitude nonlinearity, that is, a SAM. The earliest mode-locking schemes based on SPM exclusively used a coupled cavity for this purpose. In the soliton laser (*20*), pulses compressed by the soliton effects in the coupled cavity are directly coupled back into the main laser cavity. This provides more gain for the center of the pulse. At 1.5 μm, pulses as short as four optical cycles or 19 fs have been demonstrated with color center lasers (*21*). Later, the SPM-to-SAM conversion with a coupled cavity was demonstrated for a case where no soliton effects were present (*22*). In this case, an uncompressed pulse was fed back into the main cavity. An effective SAM was obtained because SPM inside the coupled cavity generates a phase modulation on the pulse (Fig. 3) that adds constructively at the peak of the pulse in the main cavity and destructively in the temporal wings, thus shortening the pulse duration inside the main cavity. This is referred to as additive-pulse mode-locking (APM) (*23*). Although very powerful in principle, these coupled-cavity schemes have the severe disadvantage that the auxiliary cavity has to be stabilized interferometrically.

An alternative method for converting the reactive Kerr nonlinearity into an effective saturable absorber has been discovered in the Ti:sapphire laser: Kerr-lens mode-locking (KLM) (*24*). In KLM, the transverse Kerr effect produces a nonlinear lens (Fig. 3) that focuses the high-intensity part of the beam more strongly than the low-intensity part. Combined with an intracavity aperture, the Kerr lens produces less loss for high intensities and forms an effective fast saturable absorber (*25*). In this configuration, the Kerr lens is most efficiently used for pulse formation if the cavity is configured to support only pulsed operation and to prohibit continuous operation of the laser. A concise account of the SAM produced by the Kerr lens in different cavity regimes can be found in (*26*). The longitudinal Kerr effect also contributes to the pulse-shaping action inside the cavity, which is well known and has been used before in dye lasers. To a good approximation, the interplay of linear and nonlinear pulse-shaping effects has been explained theoretically using Haus' master equation (*27*). This aproximation works well for longer pulses. In the sub–10-fs regime however, pulse-shaping processes become very complex (*28*), and significant deviations from this simple theoretical picture are observed.

The Kerr effect is strong enough to sustain mode-locking but is typically unable to initiate it. To overcome this limitation, an ultrabroadband SESAM can be used to reliably start KLM (*7*). With the additional stabilization mechanism provided by the SESAM, resonator alignment constraints required for pure KLM are considerably relaxed. Therefore, use of the SESAM results in a cleaner spatial mode pattern (Fig. 5). This example shows how suitable nonlinear optical effects can be used in a combination of saturable absorbers that covers several orders of magnitude of pulse duration, decoupling start-up and steady-state pulse formation.

Continuum-Generation and Amplification-Based Schemes

Independent from the generation of ultrashort pulses directly from a laser oscillator, there are schemes that generate even shorter pulses by using pulse compression outside a cavity with either standard glass fibers (*9*) or noble-gas filled, hollow fibers (*10*), and by optical parametric amplification of white-light continuum pulses (*8*). These schemes rely on white-light continuum generation, which was first observed with orange amplified dye laser pulses (*29*). The resulting spectrally broadened pulses spanned over the entire visible range. Structurally, there is an important difference between the compression/amplification schemes (Fig. 4, B and C) and the direct generation in an oscillator (Fig. 4A). Whereas the direct approach of generating pulses inside the oscillator performs all steps inside the laser feedback loop, the other approaches put all processes into a linear sequence.

Continuum-based schemes start with pulses from a Ti:sapphire oscillator, which are typically amplified to >100 μJ pulse energy. To date, spectral filtering due to the limited bandwidth of the gain material has prohibited the direct generation of amplified pulses with less than 16 fs duration (*30*). To achieve a

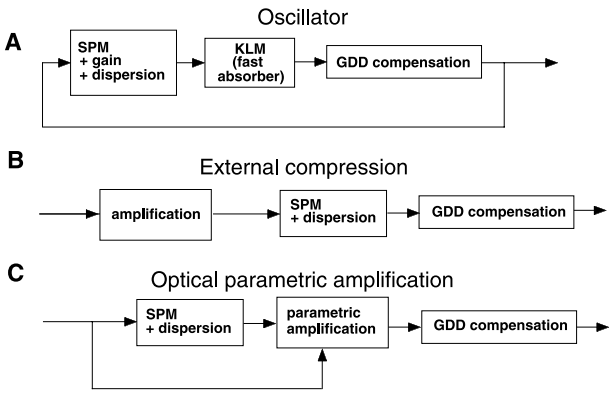

Fig. 4. Different combinations of amplification, the Kerr effect, and dispersion used for the generation of pulses in the two-cycle regime: (**A**) directly in an oscillator, (**B**) using external compression in hollow, gas-filled fibers or fused silica fibers, and (**C**) continuum generation in sapphire and subsequent parametric amplification.

bandwidth supporting two-cycle pulses, SPM is employed by focusing the amplified pulses into a nonlinear optical medium.

Noble gases such as Ar or He provide SPM with minimal dispersion. With no vibrational infrared resonance present, noble gases provide much flatter spectral dispersion than bulk materials if the same amount of SPM is desired. Additionally, they are not subject to the Raman effect, which poses another limit to the usefulness of nonlinear optical materials for SPM-based pulse compression. Because SPM is also much weaker in gases than in bulk media, higher intensities or longer interaction lengths are typically required, which is suitably provided in a strongly confined hollow-fiber geometry (*31*). Use of hollow fibers for pulse compression has produced pulses of about 4.5 fs duration. Nevertheless, similar pulse durations have been obtained in the 100-nJ pulse energy regime with standard optical fibers (*9*). The direct use with oscillators has not yet been demonstrated, and it remains to be seen how far nonlinear optical materials can be optimized and engineered for pulse compression purposes.

Frequency-conversion in nonlinear optical crystals can also be used for the generation of two-cycle pulses. Of particular interest are so-called parametric processes, which have been demonstrated with amplification bandwidths of up to 150 THz (*32*). In the parametric process, each pump photon is split into two photons, with the sum of the generated photon energies equal to the pump photon energy. If photons within the wavelength range of the parametric process are provided as a seed, they will be amplified in the nonlinear crystal. The seed pulse is derived from white-light continuum generation. Broadband parametric amplification produced pulses with a duration of <5 fs (*8*). Pumped by a frequency-doubled pulse from a Ti:sapphire amplifier system, optical parametric amplifiers (OPAs) generate sub–10-fs duration in the spectral range from 550 to 780 nm. An OPA system has been developed with microjoule pulses tunable from 1.1 to 2.6 μm and pulse durations as short as 14.5 fs (*33*).

Parametric conversion gives access to two-cycle pulses outside the spectral range of Ti:sapphire. Combination of several OPA processes seeded by the same continuum pulse allows the simultaneous generation of coherent radiation over the entire spectrum from 400 nm to 1.5 μm. This spectrum could potentially produce a single-cycle pulse (*34*), provided that dispersion compensation over such a broad range is accomplished. All continuum-based schemes require precise dispersion control, which in all cases demonstrated has been achieved using specially designed mirrors and prism sequences.

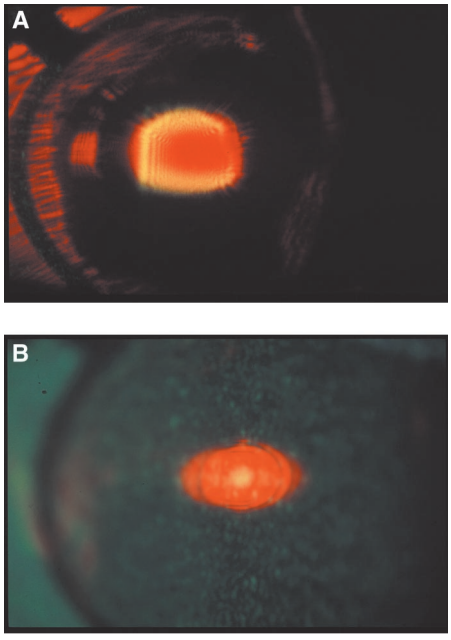

Fig. 5. Visible part of the spatial beam profiles behind one intracavity mirror of a two-cycle Ti:sapphire laser. (**A**) Cavity parameters are close to the stability limit, with pure KLM action. (**B**) Cavity is adjusted for a reduced KLM-effect with stronger stabilization action from the SESAM. Note the clearly visible yellow spectral content caused by SPM in the gain material, extending well beyond the Ti:sapphire gain bandwidth. Pictures were taken on 100ASA slide film (Kodak Elite).

Dispersion Compensation

Limited control of the intracavity dispersion is the main obstacle in the generation of extremely short pulses. For optimum pulse formation in a KLM laser, a small but constant intracavity dispersion is required over the full spectral content of the pulse (*27*). In a typical sub–10-fs Ti:sapphire laser, the uncompensated round-trip GDD caused by the laser crystal alone amounts to more than 100 fs delay between the long- and short-wavelength components covered by the gain material. To compensate for this group-delay dispersion (Eq. 2), a component with the opposite sign of dispersion has to be inserted into the cavity. Between these sections of opposite sign of GDD, the pulse width will be periodically stretched and recompressed from the sub–10-fs to the 100-fs range.

Different schemes for providing dispersion to compensate for material effects and self-phase modulation inside a laser cavity have been proposed. The prism compressor (*35*) is the most often employed scheme and introduces adjustable dispersion. However, generally it is only possible to compensate dispersion to the second order of Eq. 2 with a prism pair. For optimum performance of a laser, the prism material has to be carefully chosen and the total amount of material inside the cavity should be kept at a minimum. Pulse durations of about 8.5 fs have been demonstrated using only prism compensation (*36*). For shorter pulse operation, higher order dispersion has to be compensated for.

Specially designed mirrors can also be used for dispersion compensation. Standard dielectric mirrors are composed of identical quarter-wave layer pairs and provide high reflectance over a range of about 25% of the central wavelength, depending on the refractive index contrast of the layer materials employed. Outside this region, these simple mirror structures have considerable transmission. Special mirrors for dispersion compensation can be obtained by stacking quarter-wave layers optimized for different center wavelengths, such that long wavelengths are made to penetrate deeper into the mirror structure than short wavelengths as illustrated in Fig. 6A. Such mirrors are called chirped mirrors and the wavelength-dependent penetration depth provides the desired dispersion to compensate for material effects (*37*). In addition to dispersion compensation, chirped mirrors also give a much broader reflection bandwidth than standard mirrors.

A major problem in chirped mirror design arises due to multiple reflections between the chirped mirror structure and the top layer of the coating. The strong index discontinuity at this interface gives rise to unwanted interference, which results in oscillations of the group delay with wavelength. Double-chirped mirrors (DCMs) were developed to reduce such detrimental dispersion oscillations (*38*). Figure 6B shows the spectrally dependent penetration of the electromagnetic field into a broadband DCM coating. Reflectivity and dispersion characteristics of a DCM used in a Ti:sapphire oscillator are shown in Fig. 7, A and B, respectively. For comparison, the gain curve of Ti:sapphire is also shown in Fig. 7A.

The chirped mirror technology strongly reduces higher-order dispersion contributions inside the cavity and makes bandwidths up to 200 THz accessible for pulse generation. On a global wavelength scale, compensation is nearly perfect, yielding a small average value of the GDD. On a local scale, the mirrors introduce residual group delay oscillations with periods of several tens of nanometers (Fig. 7B). The magnitude of these residual dispersion oscillations increases with the bandwidth of the mirrors. For carefully optimized broadband DCMs, the peak-to-peak amplitude of these oscillations has been reduced to less than 1 fs per reflection, resulting in the small measured phase oscillation of the laser pulses shown in Fig. 7B. The combined action of SPM and dispersion provides a means of energy transfer within the pulse spectrum inside a mode-locked laser. Effectively, this concentrates energy at the minima of the group delay oscillations (*39*) as indicated by the strongly modulated spectra typical of sub–10-fs laser pulses; the pulse shape is strongly affected by the dispersion oscilla-

tions and significantly deviates from the simple picture predicted from the soliton-like pulse shaping (*7, 40*). Moreover, group delay oscillations can ultimately limit the intracavity bandwidth and the shortest achievable pulse width. Chirped mirrors with shifted dispersion characteristics can be combined to reduce the total intracavity group delay oscillations. Current research is directed to provide even broader bandwidth without detrimental dispersion oscillations.

Two different philosophies about the use of chirped mirrors have evolved. On the one hand, exclusive use of mirrors allows for very compact dispersion compensation schemes, which is of particular importance for oscillators (*41*). On the other hand, use of adjustable prisms in combination with chirped mirrors allows for continuous adjustment of dispersion. Using both prisms and chirped mirrors for dispersion compensation has the advantage that the chirped mirrors only have to compensate for higher-order dispersion ($i >$ 1 in Eq. 2). This results in a broader bandwidth of the chirped coatings (*38*). So it is no surprise, that the shortest pulses to date have been generated with a combination of mirror and prism dispersion compensation. Combination of the chirped mirror and SESAM technology should allow for dispersion compensation in ultracompact lasers (*42*).

Measurement

Measurement of the extremely short pulses described above is as much of a challenge as the generation itself. There is one problem inherent to simple autocorrelation measurements discussed in the introduction and Fig. 2: It is generally impossible to determine the exact shape of the pulse being measured in an autocorrelation. Determination of the exact pulse width requires accurate knowledge of this shape, which is particularly difficult with the fairly complex two-cycle pulses and their strongly modulated spectra. Guessing a pulse shape for the deconvolution of the autocorrelation can give rise to inconsistent or inaccurate results. In the case of Ti:sapphire lasers, a poorly motivated choice of an autocorrelation pulse shape was shown to result in durations well below 5 fs (*6, 7*). In both cases, these pulse durations are in contradiction to independently measured spectra and their respective bandwidth limits. To detect such problems, the measurement method should also provide independent tests for the consistency of the data.

With the complex pulse shapes in the sub–10-fs regime, techniques that allow retrieving the pulse phase and amplitude are mandatory for a proper characterization of any of the sources described here. One well-established method relies on additional information from spectrally resolving the autocorrelation and is called frequency-resolved optical gating (FROG) (*43*). Another method uses the autocorrelation data together with the fundamental spectrum (*9, 44*) to provide a simultaneous fit to both measurements. Whereas the characterization techniques discussed so far require the use of an iterative fitting algorithm to retrieve the phase, SPIDER (spectral phase interferometry for direct electric-field reconstruction) allows for fast, noniterative reconstruction of the pulse from the measurement of two spectra (*45*). Phase-sensitive techniques have been used extensively to characterize femtosecond laser sources and, apart from being more accurate, give more insight into the complex pulse dynamics of sub–10-fs pulses.

Baltuska *et al.* designed their dispersion compensation after having done FROG measurements on the uncompressed continuum (*9*). The duration of the resulting pulse was measured as 4.5 fs. For oscillators, pulses with duration as short as 5.9 fs have been characterized in amplitude and phase (*7, 46*). In these measurements, the residual uncompensated dispersion mainly due to the output-coupling mirror of the laser is clearly visible (Fig. 7B). The small oscillation in the central part of the spectrum stems from dispersion oscillations of the double-chirped mirrors. The advances in measurement tools have clearly contributed to the success of generating shorter and shorter pulses.

Conclusion and Outlook

Comparison of the different techniques that currently allow for pulses in the two-cycle regime identifies three essential mechanisms: an ultrafast spectral broadening mechanism, an ultrabroadband amplification process, and a dispersion compensation scheme. Self-phase modulation is the driving force to yield a short pulse, while the other two mechanisms compensate for power losses and tem-

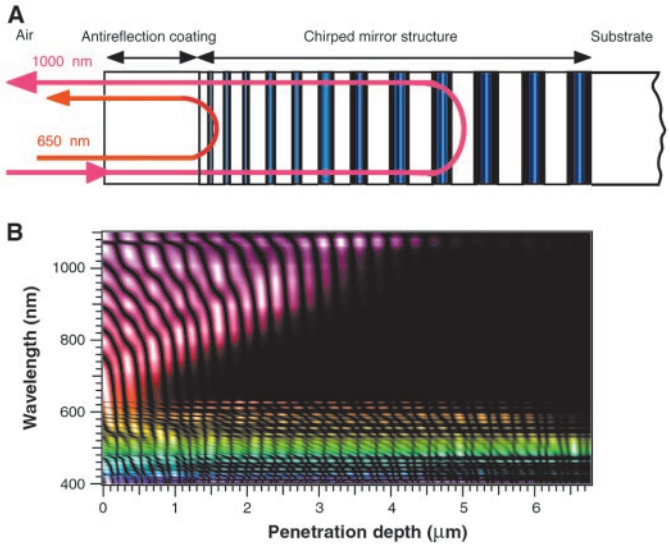

Fig. 6. Double-chirped mirror. (**A**) Structure of a typical DCM, schematically showing the path of a long-wavelength beam. (**B**) Standing-wave electric field patterns in a DCM structure versus wavelength. The dispersion of the mirrors is clearly illustrated by the dependence of penetration depth on wavelength for the range of 650 to 1050 nm. The highly transmissive region around 500 nm is used for pumping the laser.

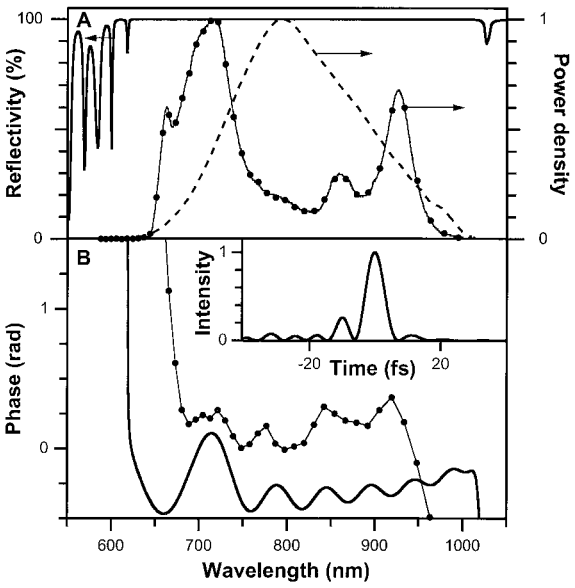

Fig. 7. (**A**) Reflectivity of a typical DCM (solid line) compared to the gain spectrum of Ti:sapphire (dashed) and the measured spectrum of a two-cycle pulse (filled circles). (**B**) Calculated phase accumulated after six reflections off a DCM and a single pass through a prism pair, as used in the external dispersion compensation (solid line) and phase of a two-cycle pulse, measured with the SPIDER technique (filled circles). The inset in (B) shows temporal intensity profile of the pulse, determined by a Fourier transform of the measured data in (A) and (B). The pulse duration is 5.9 fs.

poral pulse broadening.

The continuous improvement of femtosecond pulse sources has resulted in pulse durations of about two optical cycles, which is also close to the limit given by the bandwidth of the involved amplification and dispersion compensation processes. Compression schemes with adaptive pulse shaping (*47*) have the best prospects for further improvement in terms of pulse duration.

With the extremely short pulse durations available today, the slowly varying envelope approximation, used extensively to model nonlinear optics, is expected to break down. This approximation describes an optical pulse as a slow modulation on a high-frequency carrier wave and reduces modeling to the description of the modulation or the envelope. Experimentally, this breakdown should manifest itself in a dependence of the efficiency of nonlinear optical processes on the relative phase between the envelope and the underlying electric field of the pulse. In other words, it does matter whether the peak electric field is centered at the maximum of the intensity envelope (*48*). Recently, methods for the stabilization of the electric field structure underneath the pulse envelope with subfemtosecond accuracy were proposed (*49*).

This stabilization opens a totally new field of applications of sub–10-fs pulses. It simplifies precision optical frequency measurements that have been used for extremely accurate measurements of fundamental physical constants and could result in more precise atomic clocks (*50*). Also, there is a strong interest in phase stabilization techniques for high-harmonic generation. In this method of laser-induced coherent x-ray generation, atoms are exposed to the alternating electric field of an amplified laser source with a magnitude comparable to inner-atomic binding forces. This gives rise to the generation of a burst of x-ray pulses, potentially with attosecond (1 as = 10^{-18} s) time duration (*51*). Apart from the possible dynamic resolution, high-harmonic x-ray radiation in the 2.3 to 4.4 nm range would allow for in vivo microscopy with a good contrast between organic compounds and water (*52*). In addition, a spatial resolution of a few nanometers is possible, comparable to electron microscopy. The vision of new applications and attosecond science surely motivates today's ongoing quest for shorter laser pulses.

References and Notes

1. G. Cerullo, G. Lanzani, M. Muccini, C. Taliani, S. De Silvestri, *Phys. Rev. Lett.* **83**, 231 (1999).
2. G. J. Tearney *et al.*, *Science* **276**, 2037 (1997).
3. B. N. Chichkov, C. Momma, S. Nolte, F. v. Alvensleben, A. Tünnermann, *Appl. Phys. A* **63**, 109 (1996); J. Kruger *et al.*, *Appl. Surf. Sci.* **129**, 892 (1998).
4. J. A. Valdmanis and R. L. Fork, *IEEE J. Quantum Electron.* **22**, 112 (1986).
5. R. L. Fork, C. H. B. Cruz, P. C. Becker, C. V. Shank, *Opt. Lett.* **12**, 483 (1987).
6. U. Morgner *et al.*, *Opt. Lett.* **24**, 411 (1999); U. Morgner *et al.*, *Opt. Lett.* **24**, 920 (1999).
7. D. H. Sutter *et al.*, *Opt. Lett.* **24**, 631 (1999).
8. A. Shirakawa, I. Sakane, M. Takasaka, T. Kobayashi, *Appl. Phys. Lett.* **74**, 2268 (1999).
9. A. Baltuska, Z. Wei, M. S. Pshenichnikov, D. A. Wiersma, R. Szipöcs, *Appl. Phys. B* **65**, 175 (1997).
10. M. Nisoli *et al.*, *Appl. Phys. B* **65**, 189 (1997).
11. G. P. Agrawal, *Nonlinear Fiber Optics* (Academic Press, San Diego, CA, 1989).
12. G. I. Stegeman and M. Segev, *Science* **286**, 1518 (1999).
13. S. Sartania *et al.*, *Opt. Lett.* **22**, 1562 (1997).
14. A. E. Siegman, *Lasers* (University Science Books, Mill Valley, CA, 1986).
15. U. Keller *et al.*, *IEEE J. Sel. Top. Quantum Electron.* **2**, 435 (1996); U. Keller, in *Nonlinear Optics in Semiconductors*, E. Garmire and A. Kost, Eds. (Academic Press, Boston, 1999), vol. 59, pp. 211–286.
16. S. Gupta, J. F. Whitaker, G. A. Mourou, *IEEE J. Quantum Electron.* **28**, 2464 (1992).
17. U. Keller *et al.*, *Opt. Lett.* **17**, 505 (1992); K. J. Weingarten, U. Keller, T. H. Chiu, J. F. Ferguson, *Opt. Lett.* **18**, 640 (1993).
18. I. D. Jung *et al.*, *Appl. Phys. B* **65**, 137 (1997).
19. S. Schön, H. Zogg, U. Keller, *J. Crystal Growth* **201/202**, 1020 (1999).
20. L. F. Mollenauer and R. H. Stolen, *Opt. Lett.* **9**, 13 (1984).
21. F. M. Mitschke and L. F. Mollenauer, *Opt. Lett.* **12**, 407 (1987).
22. P. N. Kean *et al.*, *Opt. Lett.* **14**, 39 (1989).
23. E. P. Ippen, H. A. Haus, L. Y. Liu, *J. Opt. Soc. Am. B* **6**, 1736 (1989).
24. D. E. Spence, P. N. Kean, W. Sibbett, *Opt. Lett.* **16**, 42 (1991).
25. F. Salin, J. Squier, M. Piché, *Opt. Lett.* **16**, 1674 (1991); D. K. Negus, L. Spinelli, N. Goldblatt, G. Feugnet, in *Advanced Solid-State Lasers*, G. Dubé and L. Chase, Eds. (Optical Society of America, Washington, DC, 1991), vol. 10, pp. 120–124; U. Keller, G. W. 't Hooft, W. H. Knox, J. E. Cunningham, *Opt. Lett.* **16**, 1022 (1991).
26. V. Magni, G. Cerullo, S. De Silvestri, A. Monguzzi, *J. Opt. Soc. Am. B* **12**, 476 (1995).
27. H. A. Haus, J. G. Fujimoto, E. P. Ippen, *IEEE J. Quantum Electron.* **28**, 2086 (1992).
28. F. Krausz *et al.*, *IEEE J. Quantum Electron.* **28**, 2097 (1992).
29. R. L. Fork, C. V. Shank, C. Hirlimann, R. Yen, W. J. Tomlinson, *Opt. Lett.* **8**, 1 (1983).
30. K. Yamakawa *et al.*, *Opt. Lett.* **23**, 525 (1998); S. Backus, C. G. Durfee III, M. M. Murnane, H. C. Kapteyn, *Rev. Sci. Instrum.* **69**, 1207 (1998).
31. M. Nisoli *et al.*, *Opt. Lett.* **22**, 522 (1997).
32. G. M. Gale, M. Cavallari, T. J. Driscoll, F. Hache, *Opt. Lett.* **20**, 1562 (1995).
33. M. Nisoli, S. Stagira, S. De Silvestri, O. Svelto, *Opt. Lett.* **23**, 630 (1998).
34. O. Albert and G. Mourou, *Appl. Phys. B* **69**, 207 (1999).
35. R. L. Fork, O. E. Martinez, J. P. Gordon, *Opt. Lett.* **9**, 150 (1984); R. E. Sherriff, *J. Opt. Soc. Am. B* **15**, 1224 (1998).
36. J. Zhou *et al.*, *Opt. Lett.* **19**, 1149 (1994).
37. R. Szipöcs, K. Ferencz, C. Spielmann, F. Krausz, *Opt. Lett.* **19**, 201 (1994).
38. F. X. Kärtner *et al.*, *Opt. Lett.* **22**, 831 (1997); N. Matuschek, F. X. Kärtner, U. Keller, *IEEE J. Quantum Electron.* **35**, 129 (1999).
39. A. Rundquist *et al.*, *Appl. Phys. B* **65**, 161 (1997).
40. D. H. Sutter *et al.*, *IEEE J. Sel. Top. Quantum Electron.* **4**, 169 (1998).
41. L. Xu, G. Tempea, C. Spielmann, F. Krausz, *Opt. Lett.* **23**, 789 (1998).
42. R. Paschotta *et al.*, *Appl. Phys. Lett.* **75**, 2166 (1999).
43. R. Trebino and D. J. Kane, *J. Opt. Soc. Am. A* **10**, 1101 (1993).
44. J. Peatross and A. Rundquist, *J. Opt. Soc. Am. B* **15**, 216 (1998).
45. C. Iaconis and I. A. Walmsley, *IEEE J. Quantum Electron.* **35**, 501 (1999).
46. L. Gallmann *et al.*, *Opt. Lett.* **24**, 1314 (1999).
47. D. Yelin, D. Meshulach, Y. Silberberg, *Opt. Lett.* **22**, 1793 (1997).
48. I. P. Christov, *Opt. Lett.* **24**, 1425 (1999).
49. L. Xu *et al.*, *Opt. Lett.* **21**, 2008 (1996); H. R. Telle *et al.*, *Appl. Phys. B* **69**, 327 (1999).
50. T. Udem *et al.*, *Phys. Rev. Lett.* **79**, 2646 (1997); T. Udem, J. Reichert, R. Holzwarth, T. W. Hänsch, *Phys. Rev. Lett.* **82**, 3568 (1999).
51. G. Farkas and C. Toth, *Phys. Lett. A* **168**, 447 (1992).
52. P. Gibbon, *Phys. Rev. Lett.* **76**, 50 (1996).

53. We thank T. Kobayashi (University of Tokyo), A. Baltuska (University of Groningen), and M. Nisoli (Politecnico Milano) for providing the data in Fig. 2, A, B, and C, respectively. We gratefully acknowledge financial support by the Swiss National Science Foundation.